Chapter 3

Voltammetric determination of the antimalarial drug chloroquine using a glassy carbon electrode modified with reduced graphene oxide on WS_2 quantum dots

3.1 Introduction

Chloroquine (CQ), 4-(7-chloro-4-quinolylamino) pentyldiethylamine is extensively used in the treatment of sudden attacks of malaria and elimination of prophylaxis for many decades. This drug is widely used for curing rheumatoid arthritis and similar kinds of collagen diseases. CQ is also used for amoebic hepatitis treatment [Tracy et al., 1996; Weingarten et al., 1981; Thapliyal et al., 2016]. Unluckily, various strains of *Plasmodium falciparum* have developed resistance against CQ [Saad et al., 2005]. But due to its low cost, this drug is still widely used in developing countries. It is also recommended as a strong anti-cancerous agent [Savarino et al., 2006; Sotelo et al., 2006]. High doses of this drug may cause several side effects like heart attack [Muhm et al., 1996]. There are various analytical methods reported in the literature to monitor the concentration of CQ like spectrophotometric method [Qarah et al., 2017], high-performance liquid chromatography with fluorescence detection [Ducharme et al., 1997; Croes et al., 1994], chemiluminescence including radiostorage and photostoragechemiluminescence [Papadopoulos et al., 2000] and voltammetric methods [Radi, 2005]. Among all methods, voltammetric methods got immense attention due to their fast response, less volume consumption of samples, high selectivity, and sensitivity.

Graphene is an atom-thick 2D crystalline carbon film with sp^2 hybrid carbon atoms. It exhibits the unprecedented amalgamation of beneficial properties such as remarkable mechanical strength, exclusively large surface area, high thermal conductivity, and extraordinary electrical properties like tremendous charge carrier

mobility and conductivity [Jiao et al., 2009; Park and Ruoff, 2009]. Due to these peculiar material properties, graphene has grabbed significant attention and proven its applicability in the fields of sensors [Ding et al., 2015; Zhang et al., 2015], catalysis [Zhu et al., 2015], energy-storage [Kim et al., 2009], electronics [Neto et al., 2009] and optoelectronics [Liu et al., 2008]. GO possesses various hydrophilic groups like hydroxyl carboxyl, and epoxy and also renders the possibility of functionalization using covalent or non-covalent bindings. These functional groups also allow the dispersion of GO in an aqueous solution [Xiong et al., 2015]. Further, the conductivity of GO is found to be lesser than that of rGO. So, in place of GO, rGO can also be used wherever applicable [Becerril et al., 2008; Shin et al., 2009]. Utilizing the beneficial film-like structure, graphene-based composites by incorporation of graphene with diverse functional nanomaterials like metal compounds [Yin et al., 2015], noble metals [Du et al., 2014], carbonaceous materials [Zhao et al., 2015], polymeric materials [Kumar and Prakash, 2014], etc. have been prepared which showed enhanced mechanical, electrical, chemical, mechanical and catalytic properties. Consequently, varieties of sensors have been developed in the recent scenario depicting great stability, sensitivity, and selectivity [Salavagione et al., 2014; Liu et al., 2015; Srivastava et al., 2018; Chen et al., 2018; Xing and Ma, 2016; Dadkhah et al., 2016].

Apart from graphene, 2D analogues like TMDs have also been gaining attention because of their similar properties to that of graphene. 2D WS_2 nanosheet is one of the members of this family. It has 2D building blocks of S-W-S layers which are weakly bound by van der Waals forces. Because of its exclusive chemical, electronic and mechanical properties, it has been used in several fields [Yan et al., 2017; Zhang et al., 2017; Zhou et al., 2018]. However, if the size of WS_2 is controlled, 0D WS_2 QDs can be synthesized with a size in the range of 1-10 nm. Not many reports have been published

on the preparation and applications of WS_2 QDs [Gopalakrishnan et al., 2014]. In comparison to the nanosheets, QDs possess a larger active surface area and rich exposed edges which are benign to the electrocatalytic activity towards electrochemical sensing. Also, due to the luminescent properties of the dots, they have been used in the fields of sensing, bioimaging, catalysis, electronics, HER, etc. [Yang et al., 2011; Yang et al., 2012]. Coating of QDs over 2D materials can help to prevent aggregation and enhance the stability of these materials. The WS_2 QD decorated rGO sheets can act as an immensely active electrocatalyst to enhance electrode kinetics.

The paper describes the fabrication, characterization, and analytical performance of a CQ sensor based on the rGO@WS_2 QDs modified GCE by simple voltammetric techniques in PBS at pH 6. WS_2 QDs are synthesized hydrothermally and GO was synthesized by modified Hummer's method followed by reduction. The proposed sensor is highly reproducible, stable, and sensitive for the determination of CQ in the broad concentration range from 0.5 µM to 82.4 µM.

PBS aids to maintain a constant pH in an electrolytic system and they are non-toxic. It has been chosen because our desired pH of 6.0 for the experiments comes under the working pH range of PBS. Its application is advantageous since the monosodium and disodium phosphate are highly soluble in water and PBS has a very high buffering capacity.

3.2 Experimental Section

3.2.1 Chemicals and Materials

CQ phosphate was brought from Sigma, Aldrich, USA. Absolute ethanol, Na_2HPO_4, NaH_2PO_4, and DI water were purchased from Merck, India. Na_2WO_4. $2H_2O$ was brought from SRL Private Ltd. L-cysteine was procured from Merck, India. Conc.

H_2SO_4, conc. HCl, conc. H_3PO_4, distilled water, and conc. H_2O_2 were purchased from Merck, India. All other chemicals like hydrazine hydrate, graphite powder, and $KMnO_4$ were of analytical grade and used as such with no additional purification. For the analysis of CQ in the real sample, human blood samples were collected from the Institute of Medical Science, Banaras Hindu University (Varanasi, India) and stored at -4°C.

3.2.2 Preparation of WS_2 QDs

WS_2 QDs were synthesized via a hydrothermal method in a single step. Sodium tungstate dihydrate (Na_2 $WO_4 \cdot 2H_2O$) (0.25g) and L-cysteine (HO_2CCH (NH_2) CH_2SH) (0.5g) (1:2 w/w) were mixed in DI water separately and both the solutions were constantly stirred for 10-15 min. Further, the two solutions were uniformly mixed, again followed by continuous stirring for 15 min and the temperature was maintained at 40 ˚C. In the next step, 12 N concentrated HCl was added in the required amount to set pH at 3.0. To initiate the hydrothermal process, the reaction mixture was transferred to a stainless steel-lined Teflon autoclave of 100 mL capacity. Initially, the temperature was set at 120 ˚C for 2-3 hours and a further 190 ˚C for 46 h. Then, the reaction mixture was cooled down by keeping it at RT. Finally, a yellow colloidal solution of WS_2 was obtained which was poured into a dialysis bag of retained molecular weight 2000 Da. Then, the dialyzed bag was left in ideal condition for 3–4 days to get WS_2 QDs as the final product. The systematic pathways for the preparation of WS_2 QDs are illustrated in Figure 3.1.

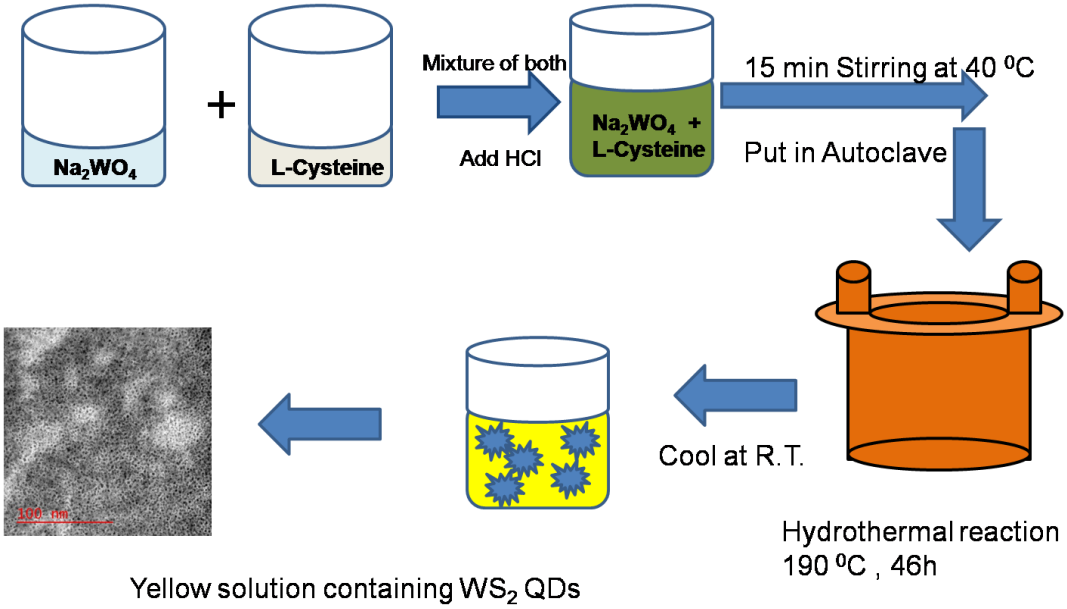

Figure 3.1 Schematic representation of the preparation of WS_2 QDs

3.2.3 Preparation of rGO

GO was synthesized with graphite powder using the well-known improved Hummer's method [Tiwari et al., 2018] with some modifications. To start with 1.5 g of graphite powder was pre-oxidized with an equal amount of $K_2S_2O_8$, and P_2O_5 (5 g each) in 40 ml of 98% H_2SO_4 at 80 °C for 4 h. Then, the obtained suspension was washed 4–5 times with DI water and the precipitate was kept at 50 °C in a vacuum oven. In the next step, pre-oxidized graphite was further oxidized by a mixture of conc. H_2SO_4 and H_3PO_4 in a 180:13 volume ratio under continuous stirring. 9 g of $KMnO_4$ was added after 5 min in the above reaction mixture. The temperature was maintained at 50 °C and the stirring was continued for 15 h. Then the reaction was stopped and left to cool down to RT. 200 mL ice was added to the reaction mixture, followed by the addition of 1.5 mL 30% H_2O_2. A U.S. standard testing sieve (pore size 30 µm) was used to separate fine material from the mixture. Thus, the obtained filtrate was centrifuged for 3 h at 5000 rpm. Sediment material was washed a number of times with DI water, HCl (30%), and

ethanol and separated by centrifugation. A suspension was made in 100 mL ether with the concluding sediment and filtered by PTFE membrane (pore size = 0.45 μm).

Afterward, to obtain rGO, the resultant suspension was sonicated again for 2 h more. At RT, hydrazine hydrate was added drop by drop in the exfoliated GO suspension in a 9:7 ratio and then reduced the mixture at 100 °C for 1 h. The resulting precipitate was filtered with cellulose filter paper and washing was done with 1 M HCl and DI water until pH reached 7. In the final step, the filtrate was dried at RT for 24 h to get rGO.

3.2.4 Preparation of rGO@WS_2QDs composite

The 1 $mgmL^{-1}$ suspension of rGO was prepared in DI water. rGO@WS_2 QDs composite was synthesized by mixing both WS_2 QDs and rGO in a 1:1 ratio by volume using a probe sonicator for 2 h at RT.

3.2.5 Preparation of modified electrode

A GCE having a geometrical surface area of 0.07 cm^2 was utilized as a substrate for the modification with rGO@WS_2QDs nanostructures. Before modification, GCE was cleaned on a wet polishing pad with 0.05 μm alumina slurry. Then it was washed 3–4 times with DI and further sonicated in DI water for 2 min for complete surface cleaning. Then, the as-prepared suspension of rGO@WS_2QDs composite was drop cast over this cleaned and polished GCE surface and allowed to dry at ambient temperature for 5–6 h and then used for all electrochemical measurements.

3.3 Results and Discussion

3.3.1 Characterization of nanomaterials by FT-IR and UV-visible spectroscopy

The interaction between WS_2 QDs and rGO was investigated with FT-IR spectroscopy. FT-IR spectra were analyzed for all three samples to justify the composite formation The FT-IR spectra of WS_2 QDs, rGO and rGO@WS_2QDs have been presented in Figure 3.2(a). A broad and strong peak at 3130–3500 cm^{-1} is attributed to the O-H and N-H stretching. A strong peak at 1635 cm^{-1} is assigned to the stretching vibration of -C=O of the carboxylic group [Zhao et al., 2018]. FT-IR of rGO was the same as earlier works reported in the literature and exhibited different types of possible functional groups where peak at 3435 cm^{-1} corresponds to O-H stretching vibration, 1635 cm^{-1} showed -C=O stretching, 1654 cm^{-1} attributed to -C=C stretching vibration, 1384 cm^{-1} assigned to -C-OH deformation vibration and a low-intensity broad band at 1040 cm^{-1} for -C-O(epoxide) vibration and -C-OH vibration of -COOH groups [Singh et al., 2017]. The characteristic peaks of both WS_2 QDs and rGO are observed in the rGO@WS_2QDs sample that elucidate the successful decoration of WS_2 QDs over rGO sheets. On comparison, the difference in the -O-H stretching vibration and the peak deviation towards longer wavelength are ascribed to the interaction among WS_2 QDs and -OH groups of rGO.

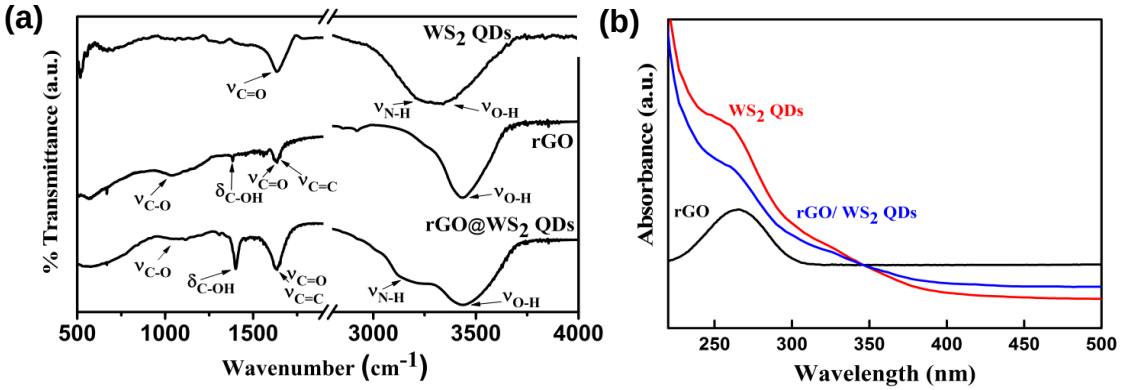

Figure 3.2 (a) FT-IR spectra and (b) UV-Vis. absorption spectra of WS_2 QDs, rGO and rGO@WS_2 QDs

Further, UV-Vis. absorption spectrum of WS_2 QDs, rGO and rGO@WS_2 QDs has been investigated and shown in Figure 3.2(b). WS_2 QDs showed two absorption peaks at 262 nm and 364 nm which were observed because of their excitonic feature. The absorption peak of rGO was found at 265 nm which endorsed the π- π^* transition in the doubly bonded carbon atoms. Further, the interactions of rGO@WS_2QDs were observed because of the quenching of peaks at 261 nm and 326 nm [Tiwari et al., 2018; Yan et al., 2016].

3.3.2 Structural characterization and elemental analysis of nanomaterials by TEM, EDAX and EDAX mapping

HRTEM was used to unravel the atomic structure of rGO, WS_2 QDs and the composite. Specimens for TEM were prepared using dilute samples by drop-casting method onto the carbon-coated TEM grids and left for complete drying for 24 h in a vacuum. TEM images of rGO (Figure 3.3a) reveal the sheet-like morphology. Single- or few-layered nanosheets of rGO are observed with plenty of wrinkles. The intrinsic nature of graphene is recommended by corrugation and scrolling. The water-soluble WS_2 QDs were characterized using TEM. The resulting TEM image demonstrates the monodispersity of WS_2 QDs (Figure 3.3b). Its structure was further verified by the SAED pattern which reveals the polycrystalline nature of WS_2 QDs. Further TEM image of rGO@WS_2QDs (Figure 3.3c) reveals that the prepared composite has the signature of the QDs distributed over nanosheets. In addition, the EDAX technique was used to investigate the presence of different elements in rGO, WS_2 QDs and rGO@WS_2QDs composite (Figure 3.4). EDAX spectra of rGO@WS_2QDs (Figure 3.4c) display the signals for Carbon, Oxygen, Tungsten and Sulphur which prove their existence in the synthesized composite. EDAX mapping was also performed to confirm

the constant distribution of all elements in the rGO@WS_2QDs composite as shown in Figure 3.5.

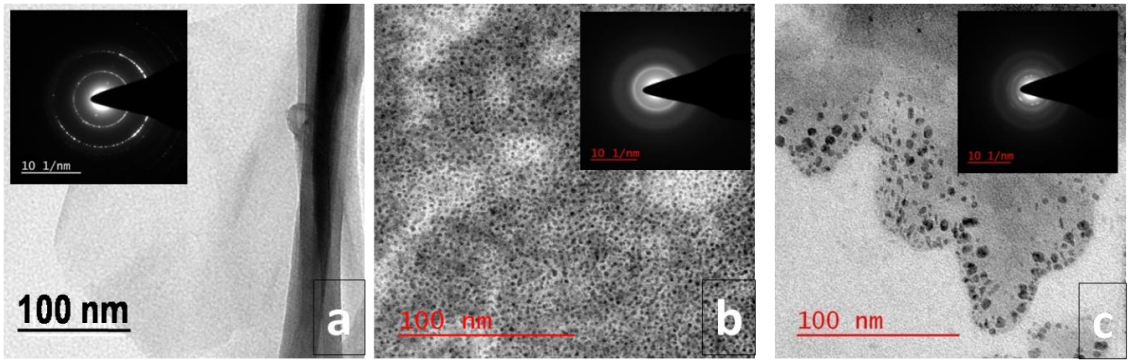

Figure 3.3 Structural investigation by TEM a) rGO b) WS_2 QDs and c) rGO@WS_2QDs (insets showing their corresponding SAED pattern)

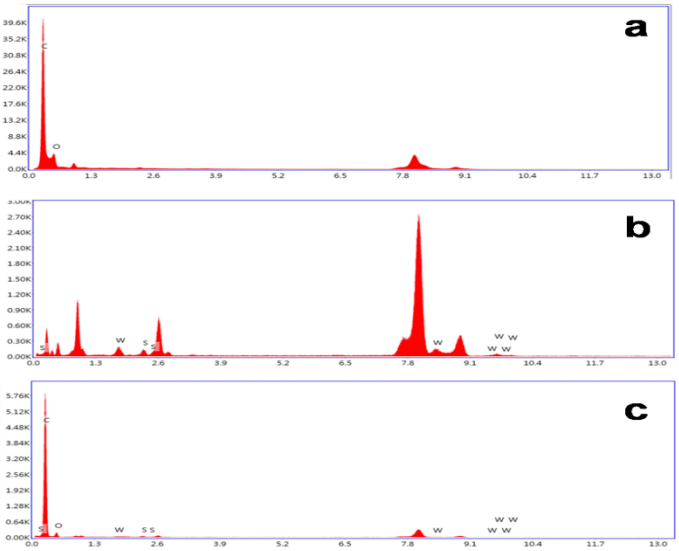

Figure 3.4 EDAX spectra of a) rGO b) WS_2 QDs and c) rGO@WS_2QDs

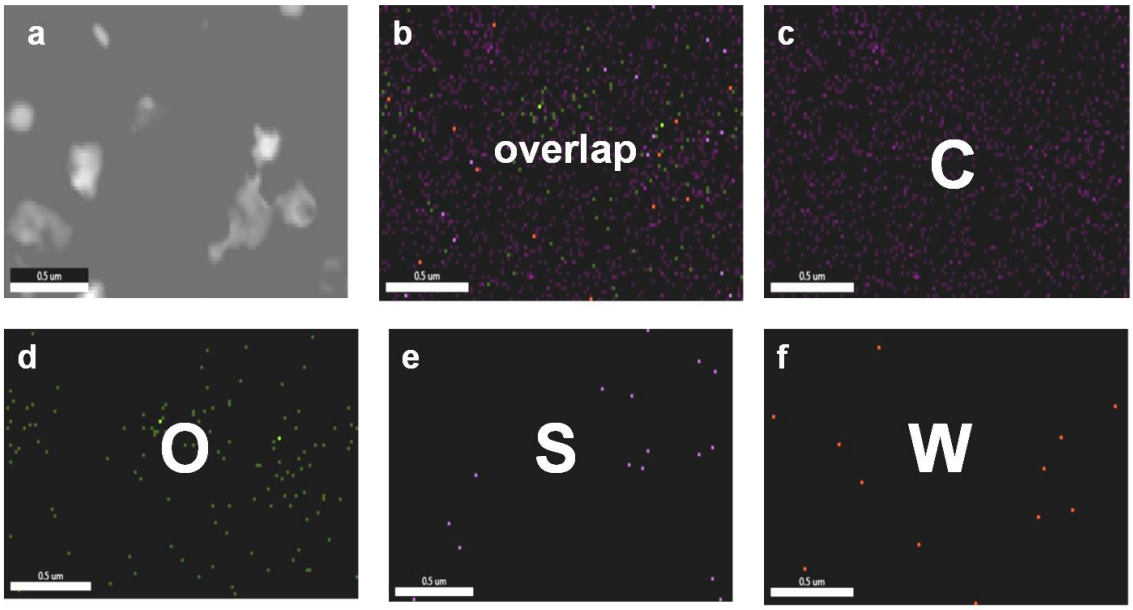

Figure 3.5 EDAX mapping for rGO@WS_2 QDs (a) TEM image of information collection area, (b) overlap, (c) C element, (d) O element, (e) S element and (f) W element

3.3.3 Comparative study of different modified electrodes towards CQ detection

To investigate the potential application of synthesized rGO, WS_2 QDs and rGO@WS_2QDs composite, a GCE was chosen and modified with different materials. Performance of different modified GCEs (WS_2 QDs modified GCE, rGO modified GCE and rGO@WS_2QDs modified GCE) were thoroughly investigated for CQ detection by CV (Figure 3.6). It is observed that in all cases CQ oxidation occurs almost at the same potential but displays different current values. The highest current response is obtained in the case of rGO@WS_2QDs modified GCE as compared to WS_2 QDs modified GCE and rGO modified GCE. This happens reasonably due to the synergistic effect of the two components.

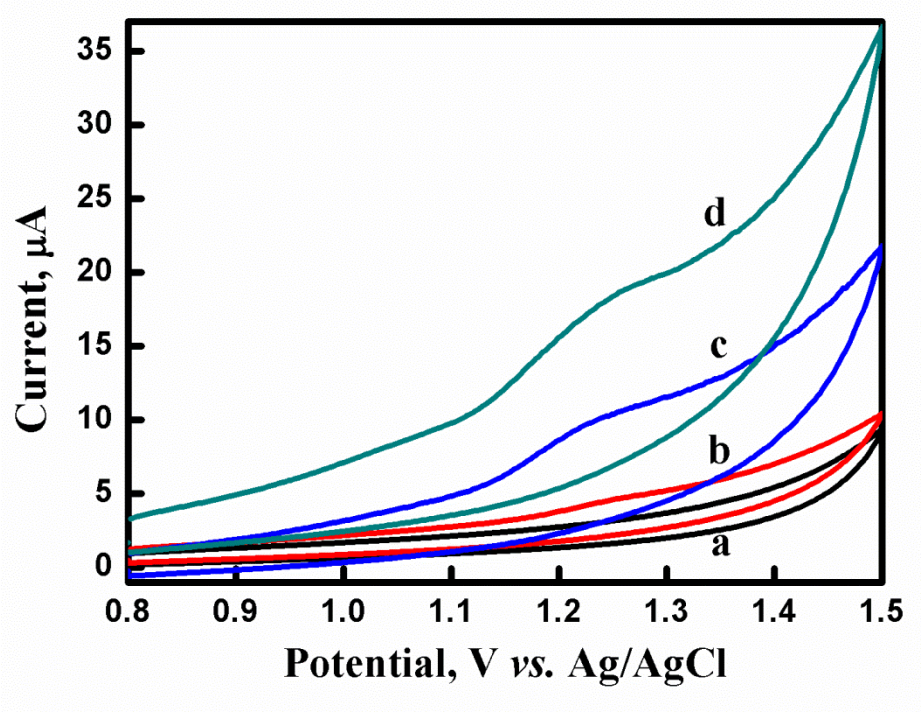

Figure 3.6 CV response of various modified electrodes in PBS (pH 6) for 50 µM CQ at (a) bare GCE, (b) rGO modified GCE (c)WS_2 QDs modified GCE and (d) rGO@WS_2QDs modified GCE.

Further CVs of CQ were recorded at a series of scan rates varying from 10 mV/s to 100 mV/s in 0.1 M PBS at bare GCE (Figure 3.7a) and rGO@WS_2QDs modified GCE (Figure 3.7b). It was revealed that in both cases, the peak current increased by an increment in the scan rate. According to the Rendles-Sevcik equation [Rafati and Afraz, 2014],

$$i_p = (2.69 \times 10^5) n^{3/2} A C D^{1/2} \upsilon^{1/2} \qquad \text{(Eq. 3.1)}$$

where i_p is the anodic peak current, n is the number of exchanged electrons, A is the surface area of the electrode (cm^2), C is the bulk concentration (mol cm^{-3}), υ is the potential scan rate (V/s) and D is the diffusion coefficient. From equation (3.1), current shows direct relation with the concentration as well as the square root of the scan rate. Keeping the CQ concentration the same, the anodic peak current i_p was plotted against

the square root of different scan rates for the bare as well as modified GCE, and a straight line was found in both cases. Figure 3.7c shows that the anodic peak current enhances linearly with the square root of the scan rate, signifying that this electrochemical process is a diffusion-controlled process. The curve suggests the faster electron transfer for rGO@WS_2QDs modified GCE as compared to bare GCE. This is attributed to a nano dimensional structure that enhances the accessible interface between the electrolytes and electrode, facilitating the electrochemical reaction over the surface of the electrode.

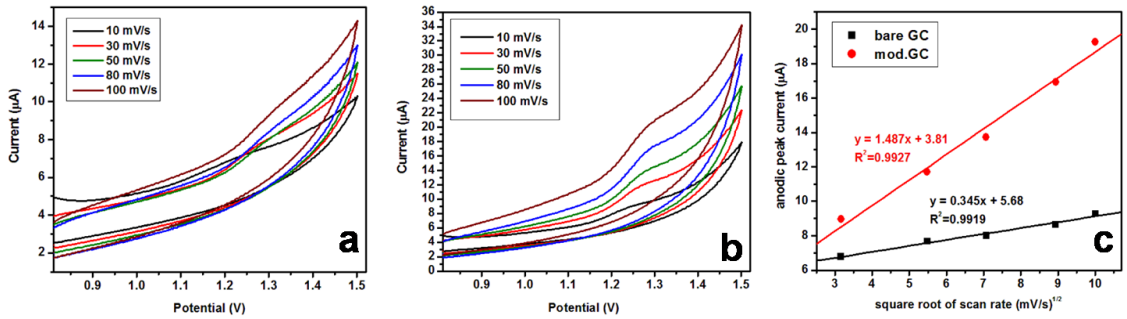

Figure 3.7 CV response of (a) bare GCE and (b) rGO@WS_2QDs modified GCE at different scan rates: 10, 30, 50, 80, 100 mV/s, in 0.1 M PBS (pH 6) in the presence of 50 µM CQ (c) Plot of anodic peak potentials vs. square root of scan rates for bare and rGO@WS_2QDs modified GCE.

3.3.4 Electrochemical sensing of CQ by CV and DPV

After optimization of various experimental conditions, electrochemical trace level detection of CQ phosphate was performed via CV and DPV techniques at rGO@WS_2QDs composite modified nanostructured platform in 0.1 M PBS (pH=6). The rGO@WS_2QDs modified GCE responds quickly towards oxidation of CQ on serial addition from 0.5 µM to 82.4 µM concentration. As the concentration of CQ increases, the anodic peak current of CQ also increases gradually which is clearly depicted in its corresponding calibration plot shown with each CV and DPV plot (Figure 3.8A, 3.8B and Figure 3.9A, 3.9B). On addition of higher concentration, peak potential is shifted

towards higher values which suggests that oxidation of CQ at a modified nanostructured platform is a diffusion-controlled process. Electrochemical sensing of CQ is performed in the linear range from 0.5 µM to 82.4 µM concentration with a regression coefficient in the order of 0.97. The LoD and sensitivity are found to be 40 nM and 0.800 $\mu A \mu M^{-1} cm^{-2}$ respectively through DPV (Figure 3.9A and 3.9B). The excellent sensitivity towards CQ detection is obtained due to larger surface area, high electroactivity and connected structures of rGO@WS_2QDs composite through various functionalities.

After successful detection of CQ at rGO@WS_2QDs modified GCE in 0.1 M PBS (pH 6), sensing was performed in human serum in order to investigate any major complications that might be related to test real samples by both CV and DPV (Figure 3.10A, 3.10B and 3.11A, 3.11B). Blood samples of a healthy and adult person were collected and blood cells were removed through centrifugation. The obtained serum was diluted five times using PBS. After dilution, the pH of the buffer was checked and there was no change in pH. The same sensing behaviour is obtained at rGO@WS_2 QDs modified GCE in serum from 0.5 µM to 82.4 µM concentration with linear calibration. The calibration plot obtained offers a LoD of 120 nM with 0.900 $\mu A \mu M^{-1} cm^{-2}$ sensitivity at S/N: 3 (Figure 3.11A and 3.11B). The same sensing behaviour in human serum also confirms the validity of the proposed sensor in other biological fluids.

CQ phosphate is a potent drug used against malaria. So, the strategy of its sensing cannot be completed before its detection in pharmaceutical formulations. For this purpose, tablets of CQ were purchased from a medical shop. A tablet of CQ was powdered using mortar and pestle and finely ground. The versatility of CQ detection was explored by acquiring the same experimental parameters as employed in ideal sensing. The same voltammetric response was obtained at rGO@WS_2 QDs modified

GCE platform on successive addition of tablet solution with a linear calibration range of 0.5 µM to 82.4 µM concentration in both CV and DPV (Figure 3.12A, 3.12B and Figure 3.13A, 3.13B). The obtained calibration plot offers good LoD as 80 nM and a sensitivity of 0.143 $\mu A \mu M^{-1} cm^{-2}$ at S/N: 3 by DPV (Figure 3.13A and 3.13B).

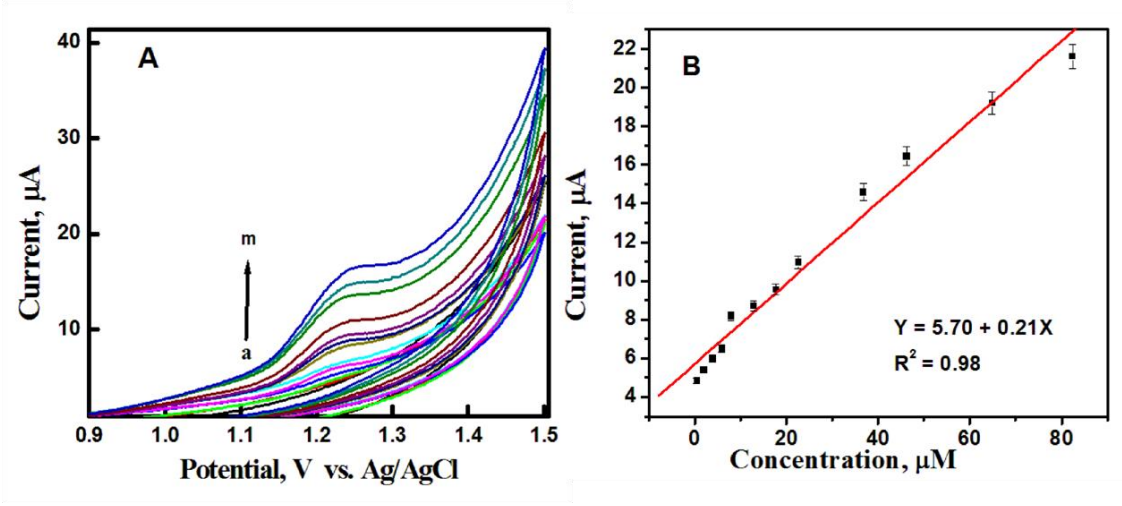

Figure 3.8 CV curve (A) and its calibration plot (B) of rGO@WS_2QDs modified GCE in the presence of CQ (0.5 µM to 82.4 µM) in 0.1 M PBS at pH=6

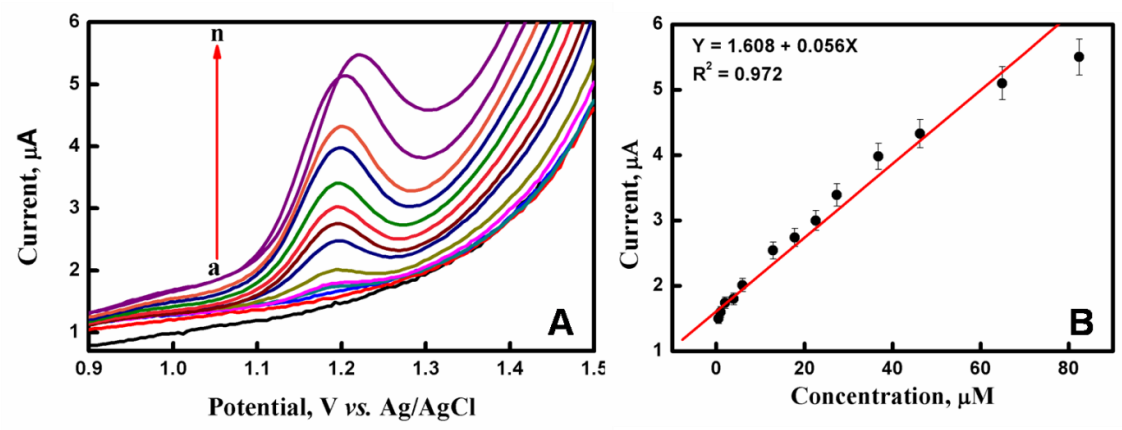

Figure 3.9 DPV curve (A) and its calibration plot (B) of rGO@WS_2QDs modified GCE in the presence of CQ (0.5 µM to 82.4 µM) in 0.1 M PBS at pH=6

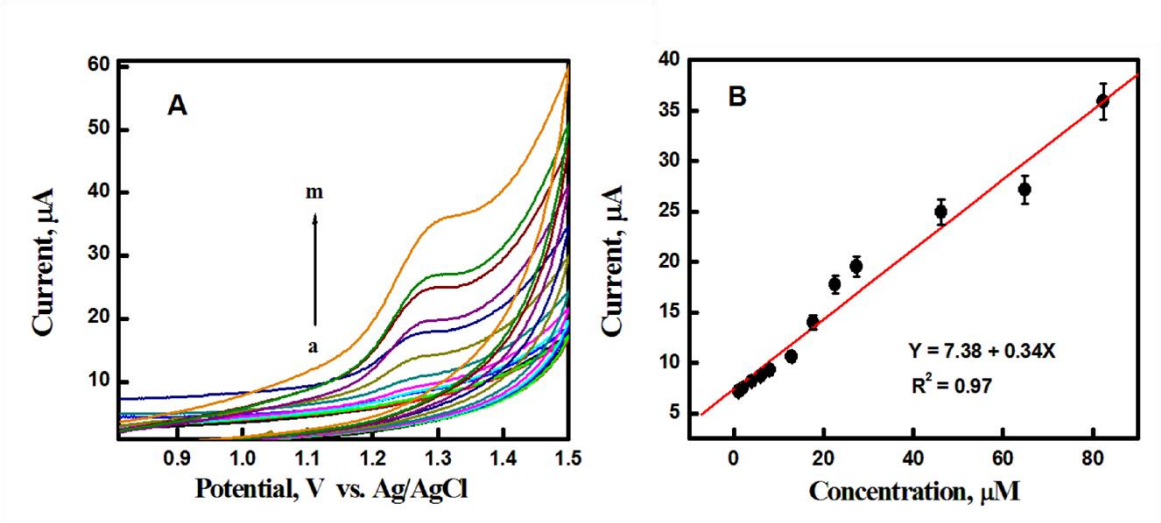

Figure 3.10 CV curve (A) and its calibration plot (B) of rGO@WS_2QDs modified GCE in the presence of CQ (0.5 µM to 82.4 µM) in human blood serum diluted with 0.1 M PBS at pH=6 in 1:4 ratio

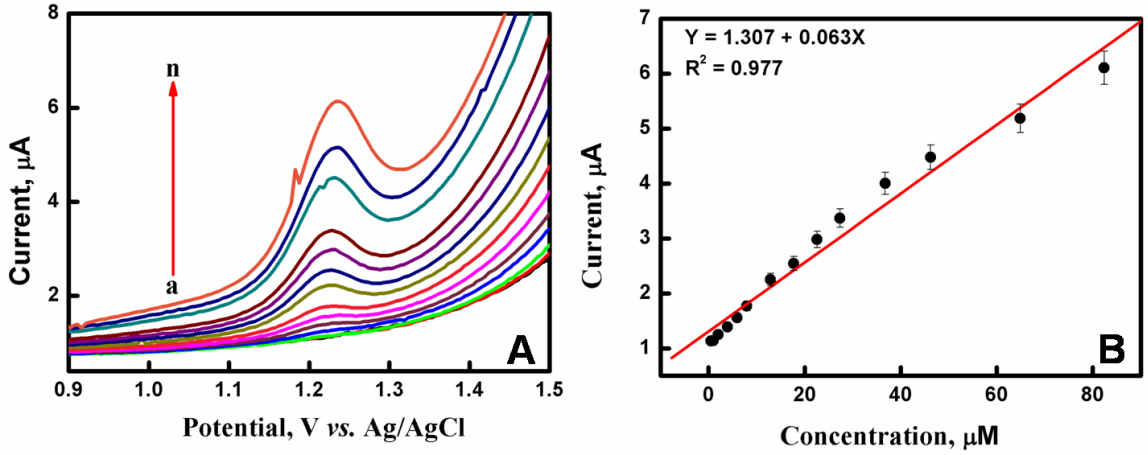

Figure 3.11 DPV curve (A) and its calibration plot (B) of rGO@WS_2QDs modified GCE in the presence of CQ (0.5 µM to 82.4 µM) in human blood serum diluted with 0.1 M PBS at pH=6 in 1:4 ratio

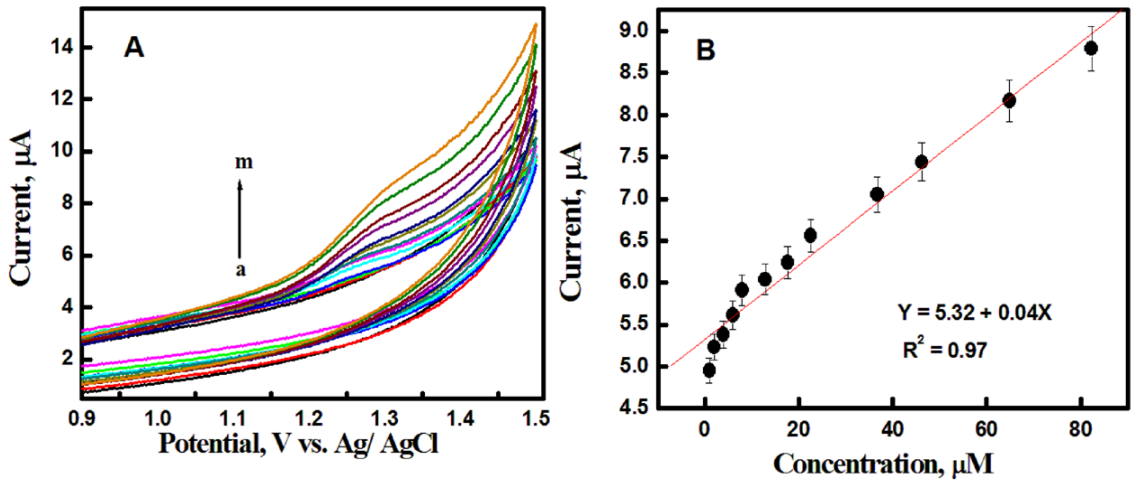

Figure 3.12 CV curve (A) and its calibration plot (B) of rGO@WS_2QDs modified GCE in the presence of commercially available CQ tablet (0.5 µM to 82.4 µM) in 0.1 M PBS at pH=6

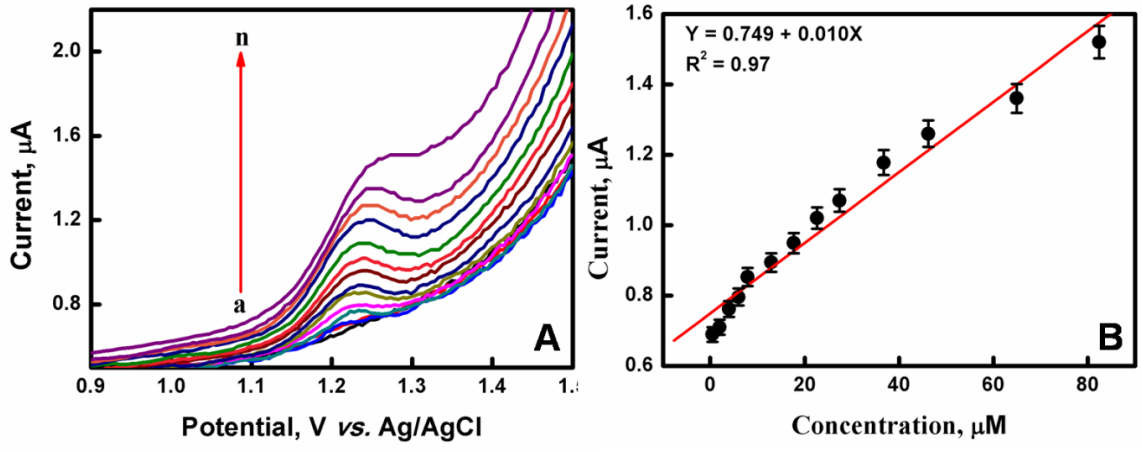

Figure 3.13 DPV curve (A) and its calibration plot (B) of rGO@WS_2QDs modified GCE in the presence of commercially available CQ tablet (0.5 µM to 82.4 µM) in 0.1 M PBS at pH=6

As seen from both CV and DPV curves, CQ is oxidized in the 1.20-1.25 V potential range, which is shown in the form of an oxidation peak. It is found that this oxidation process is irreversible, as no cathodic peak is found in CV. A plausible electro-sensing mechanism for CQ involves its electro-oxidation over rGO@WS_2QDs modified GCE as shown in Figure 3.14. The synthesized material may probably augment the conductivity of the electrode and facilitate the process of electron transfer, thereby improving the

analytical selectivity and sensitivity towards the detection of the particular analyte. Also, the high electrocatalytic efficiency of rGO@WS_2QDs facilitates a superior corridor for the electro-oxidation performance of CQ. Thus, the anodic peak shown in each DPV or CV may be ascribed to the irreversible oxidation of the *N*-heterocyclic nitrogen present in aminoquinoline moiety and the nitrogen of alkylamino side chain of CQ molecule [Radi, 2005; Mathur et al., 1990; Lama et al., 2017].

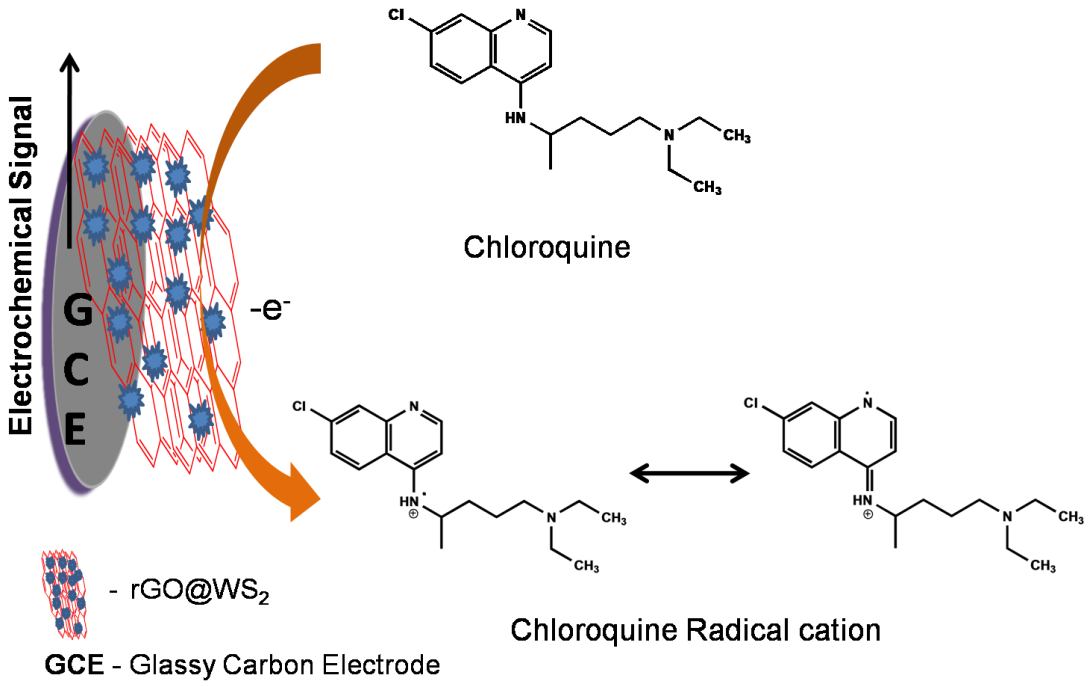

Figure 3.14 Schematic representation of plausible mechanism for electro-oxidation of CQ on rGO@WS_2QDs modified GCE

3.3.5 Interference Study:

It is well known that human blood serum has many other biocomponents, viz. carbohydrates, amino acids, lipids, salts, etc., which can interfere with desired drug detection and hinder the selectivity of proposed electrochemical sensors or biosensors. Thus, we have performed experiments with some common molecules present in human blood serum. Results described in Figure 3.15, for D-glucose, creatine hydrate, L-ascorbic acid, uric acid, L-cysteine and urea, showed very less or negligible interference

even at 10 times higher concentration of each interferent (500 µl of 1mM stock) with respect to the concentration of CQ (50 µl of 1mM stock).

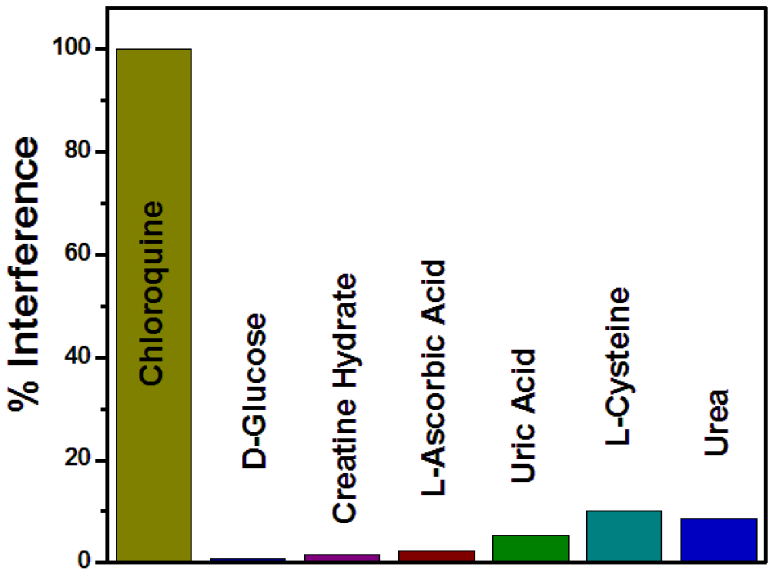

Figure 3.15 Interference studies of different biological species with CQ in the ratio of 10:1 by DPV in 0.1 M PBS at pH= 6

3.3.6 Reproducibility and Stability Study

The developed sensor can be used 2-3 times due to less change in current values as shown in Figure 3.16a. For a particular concentration of the drug, it is observed that the developed sensor showed retention of current up to 97%. After 3 h of time interval, only 2-3% current is decreased which shows that our developed sensor displays reliable stability or can be reused. On the other hand, an inter-day stability investigation of the developed sensor shows that it is highly stable for up to 10 days. More than 90% current is retained as displayed in Figure 3.16b. The electrode is highly stable towards CQ sensing and can be applied for many days with good accuracy.

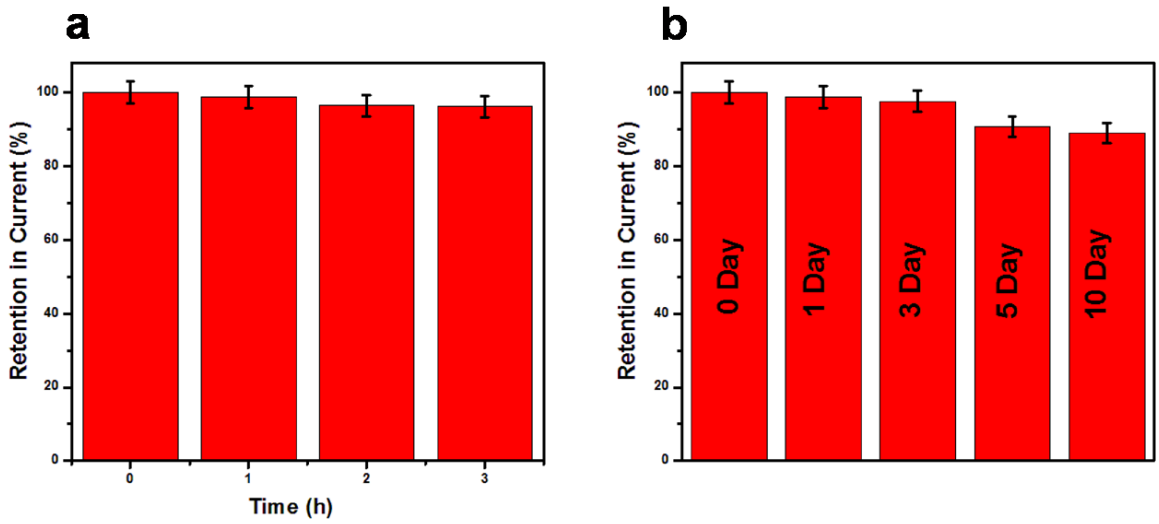

Figure 3.16 (a) Intra-day study and (b) Inter-day study of the developed electrochemical sensor by DPV in 0.1 M PBS at pH= 6 in the presence of 50 µM CQ

Our developed sensor is highly sensitive towards the detection of CQ in buffer, real samples and pharmaceutical formulations without any interference. The electrode shows reliable stability and it can be compared with other developed sensors reported earlier in the literature in Table 3.1.

Table 3.1 Comparative study for electrochemical detection of CQ based on earlier reported works

Modified Electrode	Technique	Supporting electrolyte	LoD (µM)	Linear Range (µM)	Matrix	Ref.
dsDNA/CPE	CV/DPV	B-R/ PBS	0.03	0.1-10	Spiked human serum	[Radi, 2005]
CuNW/CPE	DPV	PBS	0.02	0.13-13.3	Pharmaceutical formulation	[Mashhadizadeh et al., 2009]
rGO@WS_2QDs/GCE	CV DPV	PBS PBS	0.04 0.04	0.5 - 82.4 0.5 -	Human blood serum & Pharmaceutical formulation	Present work

				82.4	Human blood serum & Pharmaceutical formulation	
dsDNA = double stranded DNA, CuNW=$Cu(OH)_2$ Nanowire						

3.4 Conclusions

We developed a sensitive 2D materials composite modified GCE nanostructured platform for the electrochemical detection of the anti-malarial drug, CQ phosphate by two techniques, CV and DPV simultaneously. The composite serves as a nano-mediator for the rapid transfer of electrons to the electrode from the redox center. The rGO@WS_2QDs modified GCE is highly sensitive towards detection of CQ from 0.5 μM to 82.4 μM concentration range with 40 nM LoD at a signal-to-noise ratio (S/N): 3. Detection of CQ is also performed in real samples (human serum) as well as pharmaceutical formulations. Our developed sensing platform is highly reliable and sensitive for fabricating electro-sensing devices using SPEs and opens new avenues in the field of electro-sensing.